J Appl Physiol 108: 240–244, 2010.
First published October 29, 2009; doi:10.1152/japplphysiol.00615.2009.

Signals consistent with microbubbles detected in legs of normal human subjects after exercise

J. C. Wilbur,[1] S. D. Phillips,[1] T. G. Donoghue,[1] D. L. Alvarenga,[2] D. A. Knaus,[1] P. J. Magari,[1] and J. C. Buckey[2]

[1]*Creare Inc.; and* [2]*Dartmouth Medical School, Hanover, New Hampshire*

Submitted 9 June 2009; accepted in final form 28 October 2009

Wilbur JC, Phillips SD, Donoghue TG, Alvarenga DL, Knaus DA, Magari PJ, Buckey JC. Signals consistent with microbubbles detected in legs of normal human subjects after exercise. *J Appl Physiol* 108: 240–244, 2010. First published October 29, 2009; doi:10.1152/japplphysiol.00615.2009.—Exercise may produce micronuclei (presumably gas-filled bubbles) in tissue, which could serve as nucleation sites for bubbles during subsequent decompression stress. These micronuclei have never been directly detected in humans. Dual-frequency ultrasound (DFU) is a resonance-based, ultrasound technique capable of detecting and sizing small stationary bubbles. We surveyed for bubbles in the legs of six normal human subjects (ages 28–52 yr) after exercise using DFU. Eleven marked sites on the left thigh and calf were imaged using standard imaging ultrasound. Subjects then rested in a reclining chair for 2 h before exercise. For the hour before exercise, a series of baseline measurements was taken at each site using DFU. At least six baseline measurements were taken at each site. Subjects exercised at 80% of their age-adjusted maximal heart rate for 30 min on an upright bicycle ergometer. After exercise, the subjects returned to the chair, and multiple postexercise measurements were taken at the marked sites. Measurements continued until no further signals consistent with bubbles were returned or 1 h had elapsed. All subjects showed signals consistent with bubbles after exercise at at least one site. The percentage of sites in a given subject showing signals significantly greater than baseline ($P < 0.01$) at first measurement ranged from 9.1 to 100%. Overall, 58% of sites showed signals consistent with bubbles at the first postexercise measurement. Signals decreased over time after exercise. These data strongly suggest that exercise produces bubbles detectable using DFU.

ultrasound; tissue micronuclei; decompression sickness

IN THE 1940S, Harvey (14) demonstrated that bubbles do not develop in blood in a container outside the body at the levels of decompression that readily produce bubbles in the bloodsteam. Ferris et al. (12) showed that the number of men who developed decompression sickness (DCS) in their lower limbs increased while performing step (stair climbing) exercises at simulated altitude. Exercise before altitude exposure in frogs increased bubble formation substantially at altitude compared with unexercised frogs (24). By contrast, acute adynamia (e.g., by sitting) decreases the incidence of altitude DCS in humans markedly (9, 12, 13). These studies show that some factor develops during physical activity and decays with inactivity. The most likely explanation is that small nuclei (possibly gas filled) are created in tissue during exercise and serve as nucleation sites to allow for bubble formation during decompression (15).

Address for reprint requests and other correspondence: J. C. Buckey, Jr., Dartmouth Medical School, One Medical Center Dr., Lebanon, NH 03756 (e-mail: jay.buckey@dartmouth.edu).

There is indirect, but compelling, evidence that micronuclei exist and that their numbers can be affected by various factors. Evans and Walder (11), Vann et al. (23), and Daniels et al. (8) utilized hydrostatic compression (of water-breathing animals) or gas compression (of gas-breathing rats) to suppress DCS, presumably by crushing the tissue nuclei. Experiments using crabs as subjects demonstrated a resistance to the formation of visible decompression gas bubbles (seen through the carapace) when the feet of the crabs were stabilized with epoxy adhesive (20). A similar decompression when the legs were no longer immobilized produced numerous visible gas bubbles. The origin of these micronuclei is not clear, and various theories about their origin exist. The two predominant theories of micronuclei origin are metabolically generated carbon dioxide bubbles (14) and tribonucleation (the generation of bubbles by friction as one surface rubs against another) (16).

To date, however, it has not been possible to confirm that exercise produces tissue micronuclei in humans, since no technology has been available to detect them. Dual-frequency ultrasound (DFU) is a resonance-based bubble-detection technique that can detect and size small (<10 μm) bubbles and so could potentially detect tissue micronuclei. With the dual-frequency approach, ultrasound is applied both at the resonance frequency of the bubble (the pump frequency) and at some much higher imaging frequency (the image frequency) (5, 7, 17–19, 21, 22). Figure 1 shows a functional diagram of the bubble-detection instrument. The pump transducer provides the ultrasonic energy that causes the bubble to resonate. When the ultrasonic energy from the image transducer hits the resonating bubble, the bubble acts as a nonlinear mixer, and a signal is produced at the sum and difference of the pump and image frequencies. These mixing signals are detected by a receive transducer, and an analysis in the frequency domain (fast Fourier transform) separates it from the other signals.

Using this technique, small bubbles (such as ultrasound contrast agent) can be readily detected in phantoms and tissue, with an excellent signal-to-noise ratio (4). In laboratory phantoms, the minimal concentration of contrast-agent bubbles that could be detected was ~500,000/ml. Additionally, bubbles produced by decompression can be detected in tissue using DFU (3, 10). The goal of the present study was to use DFU to detect bubble signals in the legs of normal human subjects before and after exercise. If these signals were found, this would provide strong confirmatory evidence for exercise-induced, gas-filled, tissue micronuclei.

MATERIALS AND METHODS

Human testing protocol. Six normal male human subjects, with ages ranging from 28 to 52 yr provided informed consent. Subjects had a normal complete blood count, comprehensive medical panel

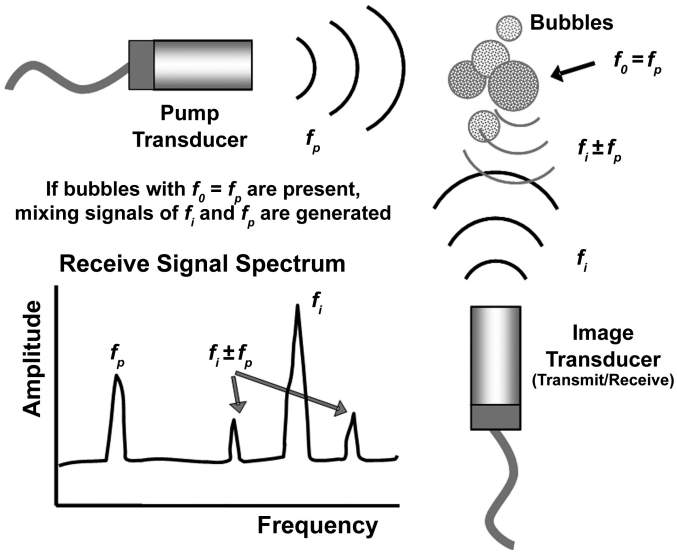

Fig. 1. Functional diagram of the bubble detector. f_0, Resonant frequency; f_p, pump frequency; f_i, image frequency. The pump frequency is selected to cause a bubble of a target size to resonate. When the image frequency strikes the resonating bubble, signal is returned at the sum and difference of the two frequencies.

(including liver tests), and ECG. A medical history (including use of prescription drugs) was taken, and a check of their vital signs was performed. Subjects were enrolled if they had a normal set of screening tests and a negative medical history (i.e., any active or past medical conditions that would increase their risk for exercise such as coronary artery disease, uncorrected congenital heart disease, cardiac arrhythmias, diabetes, pulmonary disease including exercise-induced asthma, significant connective tissue disorders, muscle disease, or malignancy).

On the morning of testing, subjects arrived at the laboratory, and their health since the screening visit was reviewed. Eleven sites were marked on the left leg (2 lateral thigh, 2 medial thigh, 2 anterior thigh, 2 anterior lower leg, 2 posterior calf, 1 posterior knee) using a Sharpie marker. Each site was imaged using two-dimensional ultrasound (Hewlett-Packard Sonos 5000). Subjects then rested in a reclining chair for a total of 2 h before exercise. For the hour before exercise, multiple baseline measurements were taken at each site using DFU. A minimum of six baseline measurements were taken at each site.

Subjects then exercised at 80% of their age-adjusted maximal heart rate for 30 min on an upright bicycle ergometer. Immediately after exercise, the subjects returned to the chair, and multiple postexercise measurements were taken at the marked sites. Measurements continued until no further signals consistent with bubbles were returned or 1 h had elapsed. The testing protocol was approved by the Committee for the Protection of Human Subjects at Dartmouth and is summarized in Fig. 2.

DFU parameters. The DFU technique has been described elsewhere (5, 17–19, 22), and is presented graphically in Fig. 1. Briefly, DFU is a low mechanical index, nonlinear, ultrasound technique that transmits two frequencies instead of one. A lower "pump" frequency (f_p) is used to drive bubbles at their resonant frequency. A second, higher "image" frequency (f_i) is transmitted as well. By adjusting the pump frequency, the size of bubble to be imaged can be selected. If a bubble of the target size is present in the measurement volume, it will be driven to resonance by the pump frequency. The resulting nonlinear oscillations, under the influence of both f_p and f_i, will cause the bubble to emit the sum $f_s = f_i + f_p$ and the difference $f_d = f_i - f_p$ of the two driving frequencies. Detection of sum and difference signals indicates the presence of bubbles of the resonant size. In this work, we focused on detecting only the difference signal.

Since native tissue micronuclei have not been detected previously, no guidance exists to choose a pump frequency for their detection, and so this was selected empirically. We chose a pump frequency of 2.25 MHz. This frequency targets spherical bubbles in the range of 1–10 μm. In previous work in our laboratory, we found this frequency works well for detecting ultrasound contrast agent (Definity, Bristol-Meyers Squibb Medical Imaging, North Billerica, MA) in tissue (3, 4) and decompression-induced bubbles in tissue (3, 10). The image frequency chosen was 5 MHz, which is a common frequency used for two-dimensional imaging ultrasound. To detect the difference between the pump and image transducers (2.75 MHz), the receive transducer was a single-element focused transducer with a center frequency of 3.5 MHz (Panametrics V382). The transducer signal was amplified to produce a voltage proportional to the received acoustic pressure. The pump transducer (Panametrics V306) was driven at a mechanical index (MI) of 0.06 (8 kPa), and the image transducer (Panametrics V309) was driven at a mechanical index of 0.04 (8 kPa). Before use, all transducers with their respective electronics were calibrated against a calibrated Onda HNR-1000 needle hydrophone.

The instrumentation used to drive the pump and image signals and to acquire and process the received ultrasound signals has been described previously (4). Two function generators (NI PXI-5401) produce the two driving signals: pump and image. These signals are each amplified using an RF power amplifier (ENI model 240L) and sent to the transmitting transducers. The receive signal is amplified (Stanford Research Systems model SR445A) by a factor of 625, filtered by a band-pass filter around the difference frequency (TTE model KC2–2.75M-10P-50-65A), and sent to a 14-bit, 100 MS/s digitizer (NI PXI-5122) set to a 16.67-MHz sampling rate. The digitizer filters the data with a high-frequency, low-pass filter before performing a fast Fourier transform. This frequency data is then sent to the LabVIEW program for analysis and display.

The transducers were positioned in a custom-made holder such that the axes of all three intersected at ~2.5 cm from the face of each transducer. The holder-unit was handheld against the subject in a manner similar to a clinical ultrasound probe. This allows for flexible positioning of transducers while maintaining the necessary alignment. The transducers were coupled to the subject using ultrasound coupling gel.

To make a measurement, the holder was placed at the marked sites on the leg, and six "interrogations" of the area of interest were made with the instrument. The pump and image transducers were activated simultaneously in a continuous wave output. To minimize electrical noise, thirty-two 1-ms samples of the received signal were collected and averaged in the frequency domain (Welch's method) to obtain a single interrogation. The transducers were turned off after the six interrogations were completed (usually ~30 s). A measurement consisted of 6 consecutive interrogations made without repositioning the transducers.

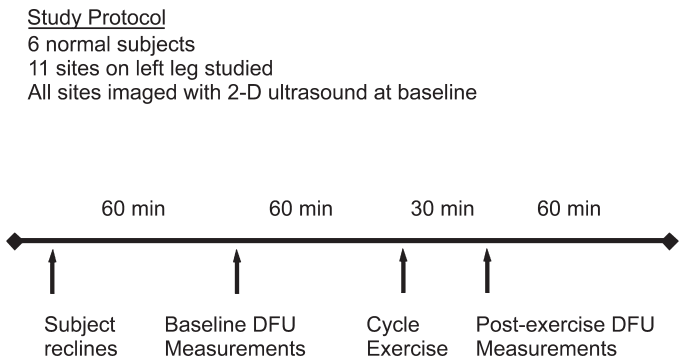

Fig. 2. Study protocol. Subjects rested in a recliner for 2 h before exercise. Dual-frequency ultrasound (DFU) measurements were taken multiple times during the hour before exercise. The subjects exercised on a cycle ergometer for 30 min, and then postexercise measurements were made.

Statistical analysis. The data were postprocessed in MATLAB. Determining statistical significance was a two-step process. First, a repeated-measures ANOVA was performed on the complete measurement set (six interrogations at each time period pre- and postexercise) for each subject at each site. This test determined whether there was a significant ($P < 0.01$) effect of time (the independent variable) on the difference signal measurements. If the ANOVA determined significance, post hoc testing was done using a Bonferroni correction for multiple comparisons. A postexercise result was determined to be positive if it was significantly different from any baseline measurement on post hoc testing. A baseline measurement was determined to be positive if it was significantly different from any other baseline measurement.

The overall number of sites that showed a positive result before exercise was compared with the overall number that showed a positive result after exercise using a χ^2 analysis.

RESULTS

Table 1 and Fig. 3 show the overall postexercise results. All the subjects had signals consistent with bubbles at at least one site after exercise. Most subjects had positive results at multiple sites. In addition, only eight baseline measurements (out of a total of 408 baseline measurements across all subjects at all sites) at seven sites were statistically different from other baseline measurements at the same site for the same subject.

The signals generally decayed over time. Figure 4 illustrates this effect from a representative site in one subject. The first two measurements after exercise were significantly different from baseline in this subject at this site. Over time, however, the signals returned back to baseline levels. The baseline levels are governed by the sensitivity threshold of the device (~170 mPa at 2.25 MHz). This threshold is governed by electrical, not acoustic, noise. Signals below this level in Figs. 4–6 can be interpreted as within the electrical noise of the system.

In general, the pattern was for signals to be detected shortly after exercise and then to decay with time. This was not a universal pattern, however. For some sites, bubbles were not detected in the first few measurements after exercise, and some time elapsed before they appeared, or they reappeared after being absent for multiple measurements. Figure 5 shows a site where strong positive signals were detected some time (~20 min in this case) after the exercise period. Approximately 15% of all sites showed this kind of pattern.

For this study, each subject served as his/her own control, and the baseline level was determined individually for each subject. This raises the possibility that signals that would be interpreted as consistent with bubbles in one subject could be baseline values in another. Figure 6 presents data to show that the signals consistent with bubbles were easily distinguished from baseline measurements. All the measurements are plotted on the same graph. The crosses and triangles show the percentage of baseline and postexercise measurements (respectively) that are above a given pressure level. There is a clear difference between the two populations. The squares show the measurements that were determined to be significantly greater than the baseline mean. In general, over all sites and subjects there was not a significant overlap in signal levels between baseline signals and signals consistent with bubbles.

Ultrasound images were taken at each measurement site, but it was not possible to standardize measurement locations precisely between subjects. The DFU measurements originate from the area where the two ultrasound beams intersect, and this could encompass a variety of anatomical structures. Also, the region of interest could vary from measurement to measurement due to transducer position and tilt. Nevertheless,

Table 1. *Overall postexercise results*

Subject	Number of Sites With Any Positive Measurement Postexercise ($P < 0.01$)	Number of Sites With a Positive First Measurement Postexercise ($P < 0.01$)
1	2	1
2	9	7
3	9	8
4	11	11
5	9	7
6	4	4
All 6 subjects	44 (67%)	38 (58%)

All values are from a total of $n = 11$ sites (or $n = 66$ sites for all 6 subjects combined).

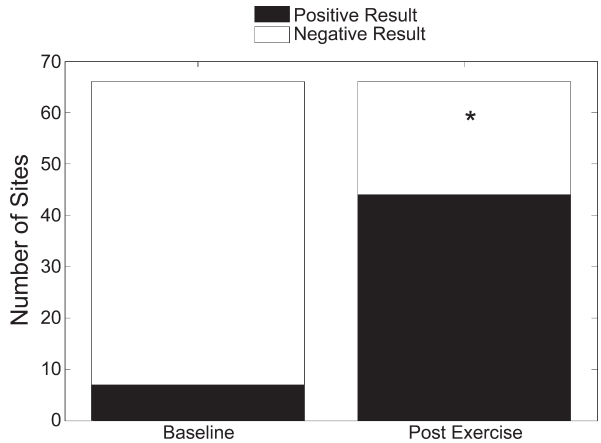

Fig. 3. Bar graph summarizing the overall results. Forty-four of 66 sites had positive signals postexercise, whereas only 7 sites had a positive baseline measurement (χ^2, $P < 0.0001$).

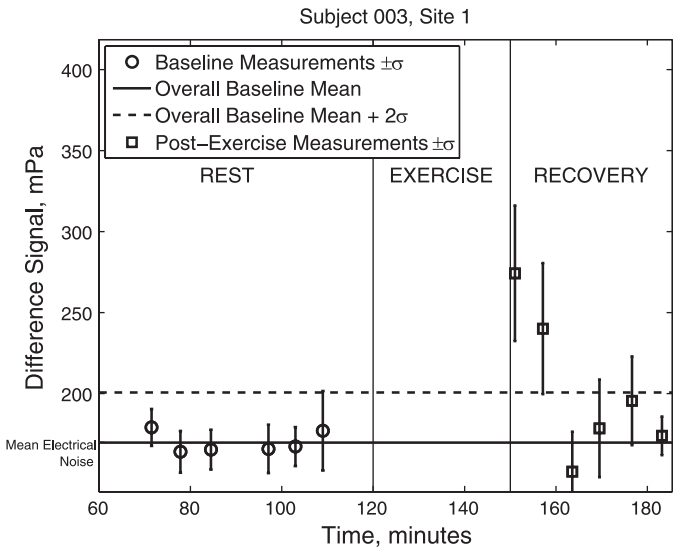

Fig. 4. Measurements from one site in one subject. Each data point consists of six consecutive interrogations at the site made without repositioning the transducers. Error bars represent ±1 SD. Positive signals were detected shortly after exercise, which decayed over time. The mean electrical noise level is at approximately the same level as the baseline mean.

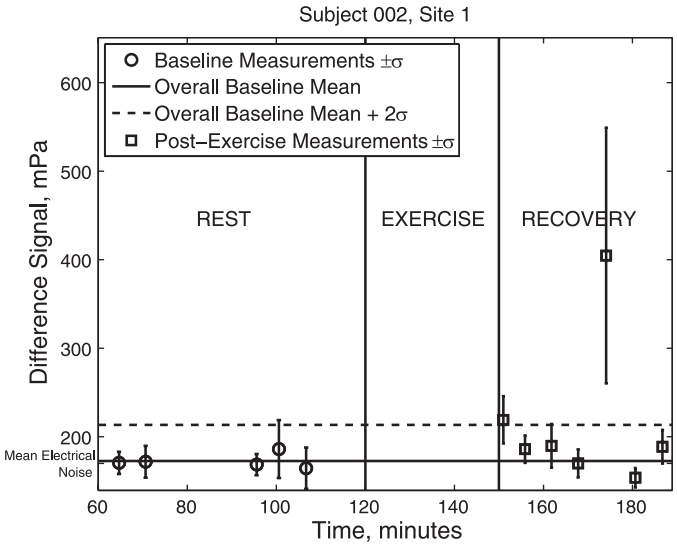

Fig. 5. Measurements from one site in one subject. Each data point consists of six consecutive interrogations at the site made without repositioning the transducers. Error bars represent ±1 SD. Positive signals were detected immediately after exercise and then again ~20 min after the exercise. The mean electrical noise level is at approximately the same level as the baseline mean. Since this noise level fluctuates, it is possible at times to detect signals with values below the mean noise level.

measurements were taken from generally similar anatomical areas on the legs of the subjects, so it was possible to identify whether some regions produced positive results more than other areas.

Table 2 shows how many subjects had positive signals at a general anatomical area postexercise. All subjects did show positive results from the upper medial aspect of the thigh, but no firm conclusions can be drawn from these results.

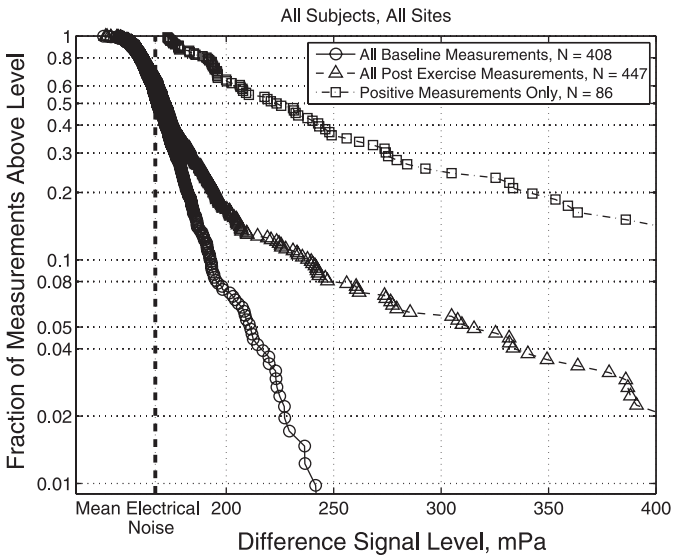

Fig. 6. Graph shows the fraction of baseline measurements (circles; $n = 408$) and postexercise measurements (triangles; $n = 447$) in all subjects at all sites above a given signal level compared with the fraction of signals consistent with bubbles (squares; $n = 86$) above a given signal level. It is clear that overall the baseline and postexercise populations are different. The plot also provides information on the expected false-positive and false-negative rates if a given threshold is chosen to determine the presence of micronuclei.

Table 2. *Subjects with positive signals at a general anatomical area postexercise*

Location	Medial	Anterior	Posterior	Lateral
Upper leg high	6	4		5
Upper leg low	2	4		4
Knee			5	
Lower leg high		5	4	
Lower leg low		3	2	

Values are the number of subjects with positive signals at a general anatomical area postexercise out of a total of $n = 6$ subjects.

DISCUSSION

In this study, we used DFU to make measurements before and after exercise at 66 sites in 6 normal human subjects. The results show that signals consistent with bubbles were returned at a majority of the sites after exercise and that the signals decayed with time after exercise. Considerable indirect evidence indicates that exercise produces tissue micronuclei, which disappear over time. These micronuclei are likely gas-filled bubbles produced by metabolism or surface forces during exercise. Since DFU is an excellent bubble detector, the best explanation for these results is that DFU is detecting exercise-induced bubbles in tissue.

DFU detects the nonlinear mixing of two ultrasonic frequencies. Bubbles are highly nonlinear oscillators, but other sources of nonlinearity can exist in tissue. As scattered pressure waves at the two transmitted frequencies co-propagate from tissue inhomogenities back to the receive transducer, they will interact with each other and may create mixing signals. The amplitudes of sum and difference signals created by nonlinear propagation are typically much less than those emitted by oscillating bubbles. We selected the transmit pressure amplitudes used in this and other work such that the mixing signal produced by this nonlinear co-propagation is just below the sensitivity threshold of the receive electronics. Nevertheless, these sum and difference signals, if present, could be interpreted as the presence of bubbles. Additionally, tissue is not a pure linear reflector of ultrasound. Tissue has nonlinear properties, which means that a small, but detectable, level of nonlinear mixing is to be expected when tissue is imaged using DFU. These sources of nonlinearity, however, should be present both before and after exercise.

One possible alternate hypothesis to explain the results from this study is that exercise may change tissue properties, and this is the explanation for the greater nonlinear signals seen after exercise. For example, exercise increases the temperature in the exercising muscle. This temperature change might influence the nonlinear properties of the tissue and lead to increased mixing signals. The amplitude of the mixing signal is directly proportional to coefficient of nonlinearity of the host material (2, 6). Data from previous studies, however, show that the change in the nonlinear parameter in tissue (B/A) is small with temperature. For instance, in breast tissue, the nonlinearity changes by only 2.4% as the temperature increases from 30 to 37°C (1). The change in difference signal amplitude from such a small change in the nonlinear coefficient would not be detected by our instrumentation in a clinical setting.

The possibility also exists that nonlinearity varies widely between individuals. Although more nonlinearity on average

was detected after exercise, if this parameter is variable, what may seem like bubbles in one subject would be interpreted as normal tissue in another. The data in Fig. 6 show that this is not the case. Although some baseline measurements had relatively high levels of nonlinearity, in general there was a sharp separation between the pre- and postexercise measurement populations. Additionally, some micronuclei may be present at baseline despite the rest period, which could produce relatively high baseline levels of nonlinearity at those sites where the micronuclei persist. Overall, there were only eight baseline measurements (over seven different sites) that were statistically different from the other baseline measurements at that same site on the same subjects.

The results from this study have important implications for DCS research and treatment. Although micronuclei have been postulated to exist in tissue, they have never been directly measured before. The ability to measure micronuclei could offer a way to examine how and where they form and their relationship to DCS risk. The ability to measure these small bubbles may be useful in diagnosing DCS and in evaluating noncompressive therapies (such as oxygen prebreathe or avoiding exercise at particular times). This technology could help to explain some of the disparate effects of exercise on DCS risk. Although some studies show increased bubble formation during decompression immediately after exercise, others show that decompression several hours after exercise (or with exercise training) reduces bubble formation (25). Also, this technology may help to understand the dynamics of bubble growth in tissue.

In this study, DFU was used to detect strong nonlinear mixers that developed after exercise. The most likely explanation for these results is that exercise produces gas-filled micronuclei (bubbles) that interact nonlinearly with the incident ultrasound. This is the first demonstration that these nonlinear mixers can be detected after exercise, and these results have important implications for DCS diagnosis and treatment.

GRANTS

This work was supported by the Office of Naval Research (ONR N00014-02-1-0406) and the National Space Biomedical Research Institute (NSBRI TD00402).

DISCLOSURES

No conflicts of interest are declared by the authors.

ACKNOWLEDGMENTS

We acknowledge the assistance we received from Lawrence A. Crum at the University of Washington Applied Physics Laboratory. His laboratory was very helpful in calibrating our transducers and in helping us with the development of the device. This work would not have been possible without the efforts of Benjamin Bollinger, who did extensive work with the bubble detector during his time at the Thayer School. We thank Richard Vann and Neal Pollock for advice and counsel as we worked through the development of this research.

REFERENCES

1. **Beyer RT.** The parameter B/A. In: *Nonlinear Acoustics*, edited by Hamilton MF, Blackstock DT. New York: Academic Press, 1998, p. 25–40.
2. **Blackstock DT, Hamilton MF, Pierce AD.** Progressive waves in lossless and lossy fields. In: *Nonlinear Acoustics*, edited by Hamilton MF, Blackstock DT. New York: Academic Press, 1998, p. 65–150.
3. **Bollinger BR.** Dual-frequency ultrasound detection and sizing of microbubbles for studying decompression sickness. In: *PhD Thesis. Thayer School of Engineering*. Hanover, NH: Dartmouth College, 2008, p. 222.
4. **Bollinger BR, Wilbur JC, Donoghue TG, Phillips SD, Knaus DA, Magari PJ, Alvarenga DL, Buckey JC.** Dual-frequency ultrasound detection of stationary microbubbles in tissue. *Undersea Hyperb Med* 36: 127–136, 2009.
5. **Buckey JC, Knaus DA, Alvarenga DL, Kenton MA, Magari PJ.** Dual-frequency ultrasound for detecting and sizing bubbles. *Acta Astronaut* 56: 1041–1047, 2005.
6. **Cain CA, Nishiyama H, Katakura K.** On ultrasonic methods for the measurement of the nonlinear parameter B/A in fluid-like media. *J Acoust Soc Am* 80: 685–689, 1986.
7. **Cathignol D, Chapelon JY, Newhouse VL.** Bubble sizing with high spatial resolution. *IEEE Trans Ultrason* 37: 30–37, 1990.
8. **Daniels S, Eastaugh W, Paton M, Smith B.** Micronuclei and bubble formation: a quantitative study using the common shrimp, crangon crangon. In: *Underwater Physiology VIII. Proceedings of the Eighth Symposium on Underwater Physiology*, edited by Bachrach AJ, Matzen MM. Bethesda, MD: Undersea Medical Society, 1984, p. 147–157.
9. **Dervay JP, Powell MR, Butler B, Fife CE.** The effect of exercise and rest duration on the generation of venous gas bubbles at altitude. *Aviat Space Environ Med* 73: 22–27, 2002.
10. **Donoghue TG, Bollinger BR, Wilbur JC, Phillips SD, Alvarenga DL, Knaus DA, Magari PJ, Buckey JC.** Decompression-induced tissue bubbles detected using dual-frequency ultrasound (Abstract). *Aviat Space Environ Med* 80: 290, 2009.
11. **Evans A, Walder DN.** Significance of gas micronuclei in the aetiology of decompression sickness. *Nature* 222: 251–252, 1969.
12. **Ferris EB, Webb JP, Ryder HW, Engel GL, Romano J, Blankenhom MA.** The Importance of Straining Movements in Electing the Site of the Bends. Washington, DC: US NRC CAM, 1943.
13. **Gray JS, Masland RL.** Studies on altitude decompression sickness: II. The effects of altitude and exercise. *J Aviation Med* 17: 483–493, 1946.
14. **Harvey EN.** Physical factors in bubble formation. In: *Decompression Sickness*, edited by Fulton JF. New York: Saunders, 1951, p. 90–114.
15. **Hempleman HV.** History of the decompression procedures. In: *The Physiology and Medicine of Diving*, edited by Bennett PB, Elliot DH. New York: Saunders, 1993, p. 342–375.
16. **Ikels KG.** Production of gas bubbles in fluids by tribonucleation. *J Appl Physiol* 28: 524–527, 1970.
17. **Leighton TG.** Acoustic bubble detection. I. The detection of stable gas bodies. *Environ Eng* 7: 9–16, 1994.
18. **Leighton TG, Lingard RJ, Walton AJ, Field JE.** Bubble sizing by the non-linear scattering of two acoustic frequencies. In: *Natural Physical Sources of Underwater Sound: Sea Surface Sound (2)*, edited by Kerman BR. Boston: Kluwer Academic Publishers, 1993, p. 453–466.
19. **Magari PJ, Kline-Schoder RJ, Stoedefalke BH, Butler BD.** A noninvasive, in-vivo bubble sizing instrument. In: *IEEE Ultrasonics Symposium*. Ontario, Canada: IEEE, 1997, p. 1205–1210.
20. **McDonough PM, Hemmingsen EA.** Bubble formation in crabs induced by limb motions after decompression. *J Appl Physiol* 57: 117–122, 1984.
21. **Newhouse VL, Shankar PM.** Bubble size measurements using the nonlinear mixing of two frequencies. *J Acoust Soc Am* 75: 1473–1477, 1984.
22. **Phelps AD, Leighton TG.** Acoustic bubble sizing using two frequency excitation techniques. In: *2nd European Conference on Underwater Acoustics*, edited by Bjorno L. Copenhagen: European Communiites, 1994, p. 201–206.
23. **Vann RD, Grimstad J, Nielsen CH.** Evidence for gas nuclei in decompressed rats. *Undersea Biomed Res* 7: 107–112, 1980.
24. **Whitaker DM, Blinks LR, Berg WE, Twitty VC, Harris M.** Muscular activity and bubble formation in animals decompressed to simulated altitudes. *J Gen Physiol* 28: 213–223, 1945.
25. **Wisloff U, Brubakk AO.** Aerobic endurance training reduces bubble formation and increases survival in rats exposed to hyperbaric pressure. *J Physiol* 537: 607–611, 2001.